

# mmLSH: A Practical and Efficient Technique for Processing Approximate Nearest Neighbor Queries on Multimedia Data

Omid Jafari  
Computer Science  
Department  
New Mexico State University  
Las Cruces, USA  
ojafari@nmsu.edu

Parth Nagarkar  
Computer Science  
Department  
New Mexico State University  
Las Cruces, USA  
nagarkar@nmsu.edu

Jonathan Montaña  
Department of Mathematical  
Sciences  
New Mexico State University  
Las Cruces, USA  
jmon@nmsu.edu

## ABSTRACT

Many large multimedia applications require efficient processing of nearest neighbor queries. Often, multimedia data are represented as a collection of important high-dimensional feature vectors. Locality Sensitive Hashing (LSH) is a very popular approximate technique for finding nearest neighbors in high-dimensional spaces. In order to find top-k similar multimedia objects, existing LSH techniques require users to find top-k similar feature vectors for each of the feature vectors that represent the query object. This leads to wasted and redundant work due to two main reasons: 1) not all feature vectors may contribute equally in finding the top-k similar multimedia objects, and 2) feature vectors are treated independently during query processing. Additionally, there is no theoretical guarantee on the returned multimedia results. In this work, we propose a practical and efficient indexing approach for finding top-k approximate nearest neighbors for multimedia data using LSH, called *mmLSH*. In *mmLSH*, we present novel strategies to find nearest neighbor objects for a given multimedia object query. We also provide theoretical guarantees on the returned multimedia results. Additionally, we present a buffer-conscious strategy to speedup the query processing. Experimental evaluation shows significant gains in performance time and accuracy for different real multimedia datasets when compared against state-of-the-art LSH techniques.

## Keywords

Nearest Neighbor Search, Locality Sensitive Hashing, High-Dimensional Search, Multimedia Indexing

## 1. INTRODUCTION

Finding nearest neighbors in high-dimensional spaces is an important problem in several multimedia applications. In multimedia applications, content-based data objects, such as images, audio, videos, etc., are represented using high-dimensional feature vectors, which are extracted using feature extraction algorithms such as SIFT [25], SURF [4], Marsyas [40] etc. Hence, searching for similar multimedia objects is converted to a nearest neighbor problem in the high-dimensional feature vector space. For low-dimensions ( $< 10$ ), popular tree-based index structures, such as KD-tree [5], SR-tree [20], etc. are effective, but for higher number

of dimensions, these index structures suffer from the well-known problem, *curse of dimensionality* (where the performance of these index structures is often out-performed even by linear scans) [9]. Instead of searching for exact results, one solution to address the *curse of dimensionality* problem is to look for *approximate* results. In many applications where 100% accuracy is not needed, searching for results that are *close enough* is much faster than searching for exact results [12]. Approximate solutions trade-off accuracy for a much faster performance. The goal of the approximate version of the nearest neighbor problem, also called *c-approximate Nearest Neighbor search*, is to return objects that are within  $c * R$  distance from the query object (where  $c > 1$  is a user-defined approximation ratio and  $R$  is the distance of the query object from its nearest neighbor).

### 1.1 Locality Sensitive Hashing

Locality Sensitive Hashing [15] is one of the most popular solutions for the approximate nearest neighbor (ANN) problem in high-dimensional spaces. Locality Sensitive Hashing (LSH) maps high-dimensional data to lower dimensional representations by using *random* hash functions. Data points are assigned to individual hash buckets in each hash function. The idea behind this approach is that closer data points in the original high-dimensional space will be mapped to the same hash buckets in the lower-dimensional projected space with a high probability. Since it was first introduced in [15], many variants of Locality Sensitive Hashing have been proposed [3, 27, 42, 13, 24, 36, 14, 16, 23] that mainly focused on improving the search accuracy and/or the search performance of the given queries. The performance/accuracy trade-off of the query is determined by a user-provided *success guarantee* (where a high success guarantee will return a result with high accuracy at the expense of faster performance and vice-versa).

### 1.2 Motivation for using LSH

Locality Sensitive Hashing (LSH) is known for two main advantages: its sub-linear query performance (in terms of the data size) and theoretical guarantees on the query accuracy. Additionally, LSH uses random hash functions which are data-independent (i.e. data properties such as data distribution are not needed to generate these random hash functions). Additionally, the data distribution does not affect the generation of these hash functions. Hence, in ap-

plications where data is changing or where newer data is coming in, these hash functions do not require any change during runtime. While the original LSH index structure suffered from large index sizes (in order to obtain a high query accuracy) [3, 27], state-of-the-art LSH techniques [13, 16] have alleviated this issue by using advanced methods such as *Collision Counting* and *Virtual Rehashing*. Thus, owing to their small index sizes, fast index maintenance, fast query performance, and theoretical guarantees on the query accuracy, in this paper, we propose to build *mmLSH* upon existing state-of-the-art LSH techniques.

### 1.3 Motivation of our work: Drawbacks of LSH on Multimedia Data Retrieval

Content-based objects are often represented by a collection of high-dimensional feature vectors. Popular feature extraction algorithms, such as SIFT [25], SURF [4] (for images), Marsyas [40] (for audio), etc., extract multiple features<sup>1</sup> that collectively represent the object of interest for improved accuracy during retrieval. Hence, if a user wants to find similar objects to a given query object, nearest-neighbor queries have to be performed for every individual feature vector representing the query object (and then these intermediate results are aggregated to find the final object results (Section 5.1)). Existing techniques treat these individual feature vectors as independent of each other, and hence cannot leverage common elements between these feature vector queries for improved query performance. Most importantly, existing techniques can only give theoretical guarantees on the accuracy of the individual feature vector queries, but not on the final object results.

### 1.4 Contributions of this Paper

In this paper, we propose a practical and efficient indexing approach for finding top-k approximate nearest neighbors for multimedia data using LSH, called *mmLSH*. Our main contributions are as follows:

- *mmLSH* can efficiently solve approximate nearest neighbor queries for multimedia data while providing theoretical guarantees on the accuracy of the query result.
- We propose a novel design that improves on the existing technique of Virtual Rehashing for faster processing.
- We provide rigorous theoretical analysis and guarantees behind *mmLSH*.
- Additionally, we present an advanced buffer-conscious strategy to speedup the processing of a multimedia query.
- Lastly, we experimentally evaluate *mmLSH*, on diverse real multimedia datasets and show that *mmLSH* can outperform the state-of-the-art solutions in terms of performance efficiency and query accuracy.

### 1.5 Paper Organization

The paper is organized as follows: In section 2, we present an overview of the works related to the problem proposed in this paper. In section 3, we discuss the key concepts and preliminaries that will better help the reader understand our

<sup>1</sup>For the Wang dataset (more details in Section 6), each image is represented by an average of 695 128-dimensional feature vectors

problem and proposed solution. The problem is formally defined in Section 4. We present our design and theoretical analysis of our proposed index structure, *mmLSH*, in Section 5. In Section 6, we experimentally evaluate *mmLSH* against state-of-the-art techniques, and finally in Section 7, we present the conclusions of our work.

## 2. RELATED WORK

Nearest Neighbor problem is an important problem for multimedia applications in many diverse domains such as multimedia retrieval, image processing, machine learning, etc. Since tree-based index structures can be outperformed by a linear scan, due to the *curse of dimensionality*, in high-dimensional spaces, approximate techniques are preferred due to their fast performance at the expense of some accuracy. In applications where 100% accuracy is not needed, this trade-off is justified, especially when the results are *good enough*. Due to the importance of the nearest neighbor problem in various domains, several diverse techniques have been proposed by researchers. These techniques can be broadly classified into three main categories: Hashing-based methods, Partition-based methods, and Graph-based methods.<sup>2</sup> Hashing-based methods can be further classified into learning-based hashing techniques and random hashing techniques. The benefit of random hashing techniques, such as Locality Sensitive Hashing [15], are that they are easy to construct, no need for training data, and easy to maintain and update. Additionally, Locality Sensitive Hashing provides a sub-linear (in terms of the data size) query performance and theoretical guarantees on the query accuracy. **Locality Sensitive Hashing and its variants:** The main idea of Locality Sensitive Hashing is to create random projections and hash data objects in these random projections such that nearby data objects in the original high-dimensional space will be mapped to the same hash bucket with a high probability (and conversely, data objects that are far apart from each other in the original high-dimensional space will be mapped to the same hash bucket with a low probability). It was originally proposed in [15] for the Hamming distance and then later extended to the popular Euclidean distance [12]. In this original work on Euclidean distance (E2LSH), instead of a single hash function (or a projection), a hash table consisted of several hash functions (represented by Compound Hash Keys) in order to reduce false positives. But this also generated false negatives. Hence several hash tables had to be used to reduce the number of false positives and false negatives, while keeping the accuracy of the query high. The main drawbacks of this approach were the size of the index structure (since large number of hash tables were required to return the desired number of results with a high accuracy) and the need to determine the width of the hash bucket during index creation (a larger width returned enough results but also with a potential of too many false positives, whereas a smaller width had a potential of misses resulting in insufficient results). This user-defined width, which was mainly dependent on the data distribution, had to be often determined through a trial and error process. LSH-Forest [3] was proposed where the compound hash-keys were hierarchically stored such that the algorithm could stop at a higher level in the tree if more results were

<sup>2</sup>We refer the reader to a recent survey paper [22] for an in-depth survey on these categories.

needed. In Multi-probe LSH [27], the authors proposed a technique to probe into neighboring buckets when more results were needed. Later, C2LSH [13] introduced two main concepts of *Collision Counting* and *Virtual Rehashing* that solved the two main drawbacks of E2LSH. In C2LSH, the authors proposed to create  $m$  base hash functions and choose candidate points based on how many times a data object collides with the query object (and hence instead of creating several hash tables of several hash functions, only 1 table of  $m$  base hash functions is needed), which reduced the size of the index structure. Additionally, in *Virtual Rehashing*, the neighboring buckets in each hash function are looked into incrementally when sufficient number of results are not found. In SK-LSH [24], the authors propose a linear ordering on the Compound Hash Keys such that nearby Compound Hash Keys are stored on the same (or nearby) page on the disk, thus reducing the total number of I/Os. QALSH [16] was later proposed that built query-aware hash functions such that the hash value of the query object is considered as the anchor bucket during query processing. Additionally, B+trees are built on each hash function for efficient lookups into neighboring buckets (which translate to range queries). QALSH utilizes the concepts of *Collision Counting* and *Virtual Rehashing*. Recently, I-LSH [23] was proposed to improve the Virtual Rehashing process of QALSH (where the range of the lookups are incremented exponentially). In I-LSH, the authors propose to increase the range of the lookups based on the distance to the nearest object (in the projected space) instead of increasing the range exponentially. In order to find the nearest object efficiently (since finding the nearest object during query processing is computationally expensive), the distances between each projected object and every other projected object in every hash function has to be calculated during the index generation process. While this technique reduces the overall I/Os, the index creation process and the cost has a prohibitively expensive cost.

In [37], authors propose an efficient distributed LSH implementation called PLSH. The authors propose several optimizations, such as bitmap-based optimization (for eliminating duplicate matches found in different hash tables) and cache-conscious hash table generation (to avoid cache misses to improve the index construction time). These optimizations are done on the original LSH design, whereas our proposed index structure *mmLSH* works on the newer C2LSH/QALSH design. Additionally, our cache-conscious optimizations are to improve the efficiency of the query processing (and hence very different). Recently, HD-Index [1] was introduced which generated Hilbert keys of the dataset objects and also stored the distances of the objects to each other to efficiently prune the results based on distance filters. Very recently, PM-LSH [43] was proposed where the idea was to estimate the Euclidean distance based on a tunable confidence interval value such that the overall query processing time is reduced.

**Query Workloads in High-Dimensional Spaces:** Until now, only two works [30, 17] have been proposed that focus on efficient execution of query workloads in high-dimensional spaces. In [30], the authors propose to efficiently execute set queries using a two-level index structure, called PSLSH, that is built upon C2LSH. The problem formulation, which is quite restrictive compared to our work, states that a point will be considered in the result set only if it satisfies a certain

user-defined percentage of the queries in the query workload. Additionally, it requires the user to input the number of hash functions to use in the query processing (thus, an underestimation can lead to low accuracy while an overestimation can lead to slower performance). The number of layers are split between the two levels based on a splitting factor which is determined by training over other datasets. In [17], the authors build a model based on the cardinality and dimensionality of the high-dimensional data to determine how to utilize the cache during query processing such that the total I/O is minimized. The main drawback of these two approaches is that they require prior information in terms of models that are generated from existing datasets. Hence the accuracy and efficiency of the index structures is determined by the accuracy of the models with respect to the dataset on which the querying is executed. Our proposed work, *mmLSH*, is very different from these previous works: most importantly, *mmLSH* does not require any training models and additionally, we provide a theoretical guarantee on the accuracy of the returned results.

### 3. KEY CONCEPTS AND PRELIMINARIES

In this section, we describe the key concepts behind LSH. We primarily use the terminologies and formulations introduced in E2LSH [12] and C2LSH [13], and then formally describe the problem that we solve in this paper.

#### 3.1 Key Concepts

**Hash Functions:** A hash function family  $H$  is  $(R, cR, p_1, p_2)$ -sensitive if it satisfies the following conditions for any two points  $x$  and  $y$  in a  $d$ -dimensional dataset  $D \subset \mathbb{R}^d$ :

- if  $|x - y| \leq R$ , then  $Pr[h(x) = h(y)] \geq p_1$ , and
- if  $|x - y| > cR$ , then  $Pr[h(x) = h(y)] \leq p_2$

Here,  $p_1$  and  $p_2$  are probabilities and  $c$  is an approximation ratio. LSH requires that  $c > 1$  and  $p_1 > p_2$ . In the original LSH scheme for Euclidean distance, each hash function is defined as  $h_{\vec{a},b}(x) = \lfloor \frac{\vec{a} \cdot x + b}{w} \rfloor$ , where  $\vec{a}$  is a  $d$ -dimensional random vector with entries chosen independently from the standard normal distribution  $N(0,1)$  and  $b$  is a real number chosen uniformly from  $[0, w)$ , such that  $w$  is the width of the hash bucket [12]. This leads to the following collision probability function [12], which states that if  $\|x, y\| = r$ , then the probability that  $x$  and  $y$  map to the same hash bucket for a given hash function  $h_{\vec{a},b}(x)$  is:  $P(r) = \int_0^w \frac{1}{r} \frac{2}{\sqrt{2\pi}} e^{-\frac{t^2}{2r^2}} (1 - \frac{t}{w}) dt$ . Here, the collision probability  $P(r)$  is decreasing on  $r$  for a given  $w$ . For a  $t$ , which is the largest absolute value of a coordinate of point in  $D$ , and for every  $b$  uniformly drawn from the interval  $[0, c^{\lceil \log_c td \rceil} w^2]$  and  $R = c^n$  for some  $n \leq \lceil \log_c td \rceil$  we have that  $h^R(x) = \lfloor \frac{h_{\vec{a},b}(x)}{R} \rfloor$  is  $(R, cR, p_1, p_2)$ -sensitive, where  $p_1 = p(1)$  and  $p_2 = p(c)$  [13].

Note that, since we are dealing with multimedia objects in our work, we follow the following terminology from the multimedia domain: given an object, feature-extraction algorithms extract multiple feature vectors for the object. Each feature vector is stored as a single point in our database. Each feature vector (or a point) consists of multiple features (i.e. each feature is equal to one dimension). For simplicity, in this paper, we refer to each feature vector as a *point* belonging to  $\mathbb{R}^d$ .

## 3.2 C2LSH Method

C2LSH [13] introduced the concepts of *Collision Counting* and *Virtual Rehashing*. In [13], authors theoretically show that two close points  $x$  and  $y$  collide in at least  $l$  hash layers with a probability  $1 - \delta$ , when the total number,  $m$ , of hash layers are equal to:  $m = \lceil \frac{\ln(\frac{1}{\delta})}{2(p_1 - p_2)^2} (1 + z)^2 \rceil$ . Here,  $z = \sqrt{\ln(\frac{2}{\beta}) / \ln(\frac{1}{\delta})}$ , where  $\beta$  is the allowed false positive percentage (i.e. the allowed number of points whose distance with a query point is greater than  $cR$ ). C2LSH sets  $\beta = \frac{100}{n}$ , where  $n$  is the cardinality of the dataset. Further, only those points that collide at least  $l$  times, where  $l$  is the collision count threshold, which is calculated as following:  $l = \lceil \alpha \times m \rceil$ , where the collision threshold percentage,  $\alpha$ , is  $\alpha = \frac{2p_1 + p_2}{1 + z}$ . Since C2LSH creates only one hash function per hash layer, the number of hash functions are equal to the number of hash layers. Hence, the terms *hash layer* and *hash functions* are used interchangeably in this paper.

Instead of assuming a *magic* radius (which traditional LSH methods did), C2LSH sets the initial radius  $R$  to 1. It is possible that with  $R = 1$ , there are not enough results for a top- $k$  query to be returned. C2LSH increases the radius of the query in the following sequence:  $R = 1, c, c^2, c^3, \dots$ . If at *level- $R$* , enough candidates are not found, the radius is increased until enough query results are found. This process is called *Virtual Rehashing*. While QALSH [16] also utilizes these concepts of Collision Counting and Virtual Rehashing to build query-aware hash functions, we found that C2LSH is much faster than QALSH (while returning very similar accuracy). We report these numbers in Section 6. Hence, we build *mmLSH* on top of C2LSH. It should be noted that our work is orthogonal to and can be built upon any state-of-the-art LSH-based techniques.

## 4. PROBLEM SPECIFICATION

In this section, we formally describe the problem we solve in this paper. Given a multidimensional database  $\mathcal{D}$ ,  $\mathcal{D}$  consists of  $n$   $d$ -dimensional points that belong to a bounded multidimensional space  $\mathbb{R}^d$ . Each  $d$ -dimensional point  $x_i$  is associated with an object  $X_j$  s.t. multiple points are *associated* with a single object. There are  $S$  objects in the database ( $1 \leq S \leq n$ ), and for each object  $X_j$ ,  $set(X_j)$  denotes the set of points that are associated with  $X_j$ , and  $|set(X_j)|$  denotes the number of points that are associated with  $X_j$ . Sometimes we abuse notation and denote by  $|X|$  the number of points in  $set(X)$ . Thus the total number of points in the database,  $n$ , is equal to  $\sum_{j=1}^S |set(X_j)|$ .<sup>3</sup>

In this paper, our goal is to provide a  $k$ -NN version of the  $c$ -approximate nearest neighbor problem for multidimensional objects. One of the complications that arises immediately is the lack of a notion of distance between sets of  $d$ -dimensional points. Without such a notion, it is not possible to formally define when two objects are nearby. A preliminary attempt to define such a distance is to compute the average of the Euclidean distances of pairs of features, i.e.,  $\frac{\sum_{x_1 \in set(X_1), x_2 \in set(X_2)} ||x_1, x_2||}{|set(Q)| \cdot |set(X_j)|}$ . However, this formula would

<sup>3</sup>In practice, different objects can be associated with different number of points. For example, if an image  $X_1$  has more details than image  $X_2$ , then a feature-extraction algorithm will extract more points for  $X_1$  than it will for  $X_2$ .

return a positive number when  $X_1$  and  $X_2$  are the same object, but clearly the distance between them should be zero. To remedy this, we propose a notion of distance called  $\Gamma$ -distance (formally defined in Section 5.2) and that depends on a percentage parameter that we denote by  $\Gamma$ . As it turns out, our  $\Gamma$ -distance is more accurate in assessing how similar two objects are. For example, if an image  $Q$  consists of two regions with equal area but different colors, then for any  $\Gamma \leq \frac{1}{2}$  the  $\Gamma$ -distance between this image and itself is equal to zero, while the above mentioned alternate distance is clearly positive. The effectiveness of this distance is due to the fact that it takes into account that two similar images have similar features in certain sub-regions, while other sub-regions may be very different.

Let us denote the  $\Gamma$ -distance between two objects  $X_1$  and  $X_2$  by  $\Gamma dist(X_1, X_2)$ . For a given query object  $Q$ , an object  $X_j$  is a  $\Gamma$ - $c$ -approximate nearest neighbor of  $Q$  if the  $\Gamma$ -distance between  $Q$  and  $X_j$  is at most  $c$  times the  $\Gamma$ -distance between  $Q$  and its true (or exact) nearest neighbor,  $X_j^*$ , i.e.  $\Gamma dist(Q, X_j) \leq c \times \Gamma dist(Q, X_j^*)$ , where  $c > 1$  is an *approximation ratio*. Similarly, the  $\Gamma$ - $k$ -NN version of this problem states that we want to find  $k$  objects that are respectively the  $\Gamma$ - $c$ -approximate nearest neighbors of the exact  $k$ -NN objects of  $Q$ .

## 5. mmLSH

In this section, we first explain the widely used existing solution, the Borda Count method, then explain the key definitions of mmLSH, and eventually proceed to explain the novel design and techniques of *mmLSH*. Throughout this section, we follow this notation: an *object*  $X_j$  is associated with *set*( $X_j$ )  $d$ -dimensional points.

### 5.1 Existing Solution: Borda Count Method

The Borda Count method [32], and its variants [31, 34] are popular techniques to aggregate results of multiple point queries to find similar objects in multimedia retrieval [6, 26, 34, 1]. Given a multimedia object query  $Q$ , *set*( $Q$ ) is the set of query points associated with  $Q$ . In order to find top- $k$  nearest neighbor *objects* of  $Q$ , the existing method is to find the top- $k'$  nearest neighbor *points* for each query point  $q_i$  (where  $1 \leq i \leq |set(Q)|$ ,  $k$  is the number of desired results by the user, and  $k'$  is an arbitrarily chosen number such that  $k' \gg k$  [1]). Once the top- $k'$  nearest neighbors of each query point  $q_i$  is found, an overall score (denoted by  $BC(X_j, Q)$ ) is assigned to each multimedia object  $X_j$  based on the depth of the points (associated with  $X_j$ ) in the top- $k'$  results for each of the point queries  $q_i$  of  $Q$ . Let us denote the top- $k'$  result set of  $q_i$  as  $res(q_i)$  (note that this set has to be sorted on the distances, i.e., the closest returned object should be at position 1 and so on). We denote the position of a returned point as  $pos$  (where  $1 \leq pos \leq k'$ ). Formally, this score  $BC(X_j, Q)$  is defined as following [1]:

$$BC(X_j, Q) = \sum_{i=1}^{|set(Q)|} \left[ \sum_{pos=1}^{k'} ((k' + 1 - pos) \cdot I(X_j, q_i, pos)) \right] \quad (1)$$

where  $I$  is the indicator function that is 1 if a *point* from  $X_j$  is returned at position  $pos$  for a query point  $q_i$ , and is 0 otherwise. Once these scores are calculated for all  $S$  objects in the database, the top- $k$  objects are returned as the  $k$  nearest neighbor objects of  $Q$ .

**Drawbacks of this approach:** There are two main drawbacks of this approach: 1) there is no theoretical guarantee for the accuracy of the returned top- $k$  result objects, and 2) all query points  $q_i$  of the query object  $Q$  are executed independently of each other. Hence, if a query point takes too long to execute as compared to others, then the overall processing time is negatively affected. This is especially disadvantageous if the top- $k$  results could have been found before all query points have found their respective top- $k'$  nearest neighbors.

## 5.2 Key Definitions of mmLSH

We first explain the key definitions that help us present the design of *mmLSH*. We use the following notations:  $R$  is the given radius and  $\|q_i, x_i\|$  denotes the Euclidean distance between two  $d$ -dimensional points  $q_i$  and  $x_i$ . We also use notations from [13] (that are explained in Section 3). We say  $q_i$  and  $x_i$  are *Nearby Points* if  $\|q_i, x_i\| \leq R$ .

In order to define two *Nearby Objects*, we first define a similarity/distance measure between two objects in the context of Approximate Nearest Neighbor search. Note that, there have been several works that have defined voting-based similarity/distance measures between two multimedia objects, especially images [45, 18, 44, 19]. While we do not follow any particular prior work's definition, our proposed index structure *mmLSH* is orthogonal to these approaches and can work with any of the above similarity/distance measures. Given a similarity/distance measure, the goal of *mmLSH* is to efficiently process a query workload while providing theoretical guarantees.

**DEFINITION 5.1** ( $R$ -OBJECT SIMILARITY). *Given a radius  $R$ , the  $R$ -Object Similarity between two objects  $Q$  and  $X_j$ , that consists of  $set(Q)$  and  $set(X_j)$   $d$ -dimensional feature vectors respectively, is defined as:*

$$sim(Q, X_j, R) = \frac{|\{q \in set(Q), x_i \in set(X_j) : \|q, x_i\| \leq R\}|}{|set(Q)| \cdot |set(X_j)|} \quad (2)$$

Note that,  $0 \leq sim(Q, X_j, R) \leq 1$ .  $sim(Q, X_j, R)$  will be equal to 1 if every point of  $Q$  is a distance at most  $R$  to every point of  $X_j$  (e.g. if you are comparing an entirely green image with another green image - and assuming the feature vectors were based on the color of the pixel points. But if you are comparing two identical images such as a bus, then  $sim(Q, X_j, R) < 1$  if  $R$  is less than the largest among  $\|q, x_i\|$ , since a subset of feature vectors representing a wheel will not be close to a subset of the feature vectors). Since the number of points associated with two objects can be different, we normalize the similarity with respect to the number of points associated with  $Q$  and  $X_j$ .

We are now ready to present our proposed notion of distance between two sets of  $d$ -dimensional points.

**DEFINITION 5.2** ( $\Gamma$ -DISTANCE). *Given a two objects  $Q$  and  $X_j$ , that consists of  $set(Q)$  and  $set(X_j)$   $d$ -dimensional feature vectors respectively, the  $\Gamma$ -distance between  $Q$  and  $X_j$  is defined as:*

$$\Gamma dist(Q, X_j) = \inf\{R \mid sim(Q, X_j, R) \geq \Gamma\} \quad (3)$$

In order to find points that are within  $R$  distance, we use the *Collision Counting* method that is introduced in C2LSH [13]: given a query point  $q$  and  $m$  projections, a point  $x$  is

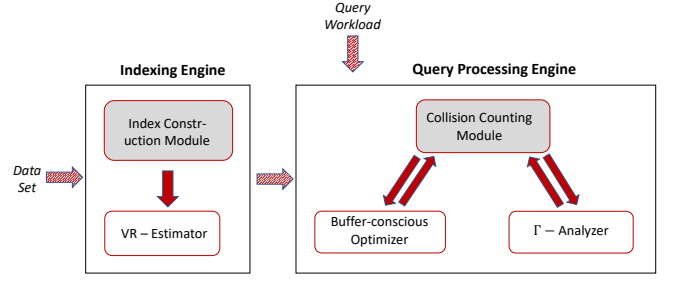


Figure 1: Architecture of *mmLSH*

considered a *candidate* if  $x$  collides with  $q$  (also called the *collision count*) in at least  $l$  projections (see Section 3.2). [13] proves that if  $\|q, x\| \leq R$ , then the collision count of  $x$  with respect to  $q$  (denoted by  $cc(q, x)$ ) will be at least  $l$  with a success probability of  $1 - \delta$ .

We define a *Collision Index* (denoted by  $ci(Q, X_j)$ ) that determines how close two objects are based on the number of points between the two objects that are considered *close* (i.e. the collision counts between the points of the two objects is greater than the collision threshold  $l$ ).

**DEFINITION 5.3** (COLLISION INDEX OF TWO OBJECTS). *Given two objects  $Q$  and  $X_j$ , that consists of  $set(Q)$  and  $set(X_j)$  feature vectors respectively, the collision index of  $X_j$  with respect to  $Q$  is defined as:*

$$ci(Q, X_j) = \frac{|\{q \in set(Q), x_i \in set(X_j) : cc(q, x_i) \geq l\}|}{|set(Q)| \cdot |set(X_j)|} \quad (4)$$

The *Collision Index* between two objects depends on how many nearby points are considered as candidates between the two objects. Thus, in turn, the accuracy of the collision index depends on the accuracy of the collision counting process (i.e. if two points are *nearby*, then the collision count between these two points should be greater than the collision threshold  $l$ ). [13, 16] have already shown experimentally that the accuracy of the collision counting technique to be very high. Hence we define an object  $X_j$  to be a  $\Gamma$ -candidate if the collision index between them is greater than or equal to  $(1 - \varepsilon)\Gamma$ , where  $\varepsilon > \delta$  is an approximation factor which we set to  $2\delta$ .

**DEFINITION 5.4** ( $\Gamma$ -CANDIDATE OBJECTS). *Given an object query  $Q$  and an object  $X_j$ , we say that  $X_j$  is a  $\Gamma$ -candidate with respect to  $Q$  if  $ci(Q, X_j) \geq (1 - \varepsilon)\Gamma$ .*

Additionally, we define an object to be a  $\Gamma$ -false positive if it is a  $\Gamma$ -candidate but its  $\Gamma$ -distance to the object query is too high.

**DEFINITION 5.5** ( $\Gamma$ -FALSE POSITIVES). *Given an object query  $Q$  and an object  $X_j$ , we say  $X_j$  is a  $\Gamma$ -false positive with respect to  $Q$  if we have  $ci(Q, X_j) \geq \Gamma + \frac{\varepsilon}{2}$  but  $\Gamma dist(Q, X_j) > cR$ .*

## 5.3 Design of mmLSH

The main goal of *mmLSH* is to *efficiently* return more accurate top- $k$  objects for a given query object while providing theoretical guarantees on the accuracy of the result. Figure 1 shows the workflow and the architecture of *mmLSH*. In this

figure, the modules (rectangles) that are grey-highlighted use existing state-of-the-art techniques (C2LSH). Note that, while *mmLSH* can be built on top of any state-of-the-art LSH-based techniques, we build *mmLSH* on the state-of-the-art technique C2LSH [13]. Once the *Indexing* engine indexes the dataset, we run our *VR-Estimator* (Section 5.4) to find a better starting radius for the query processing. The constructed index and the improved starting radius are then used in the *Query Processing* engine.

During query processing, instead of executing the query points of  $Q$  independently, we execute them one at a time in each projection (Lines 9-10 in Algorithm 1). In Alg. 1, the function *CountCollisions*( $q_i$ ) (Line 11), an existing function from C2LSH, is responsible for counting collisions of query points and points in the database and updating the pointers of the range searches in the projections [13]. This function is represented by the *Collision Counting* module in Fig. 1.

The *Buffer-conscious Optimizer* module (Section 5.5) is responsible for finding an effective strategy to utilize the buffer to speed up the query processing. This module decides which query and the hash bucket should be processed next. The  $\Gamma$ -Analyzer module is in charge of calculating the *collision indexes* (Section 5.2) for objects in the database and for checking/terminating the process if the terminating conditions are met (Section 5.3.1).

### 5.3.1 Terminating Conditions for *mmLSH*

We first explain the terminating conditions used by *mmLSH*. The existing solution (Section 5.1) finds top- $k'$  candidates for each query point in  $Q$  and then terminates. Instead, *mmLSH* stops when top- $k$  objects are found. The following are the two terminating conditions in *mmLSH*:

- T1) At certain point at level- $R$ , at least  $k + \beta S$   $\Gamma$ -candidates have been found, where  $\beta S$  is the allowed number of false positives. (Line 14, Alg. 1)
- T2) At the end of level- $R$ , there exists at least  $k$   $\Gamma$ -candidates whose  $\Gamma$ -distance to  $Q$  is at most  $cR$ . (Line 6, Alg. 1)

Naturally, the terminating conditions of *mmLSH* are dependent on  $\Gamma$ . These terminating conditions guarantee that  $\Gamma$ - $c^2$ -approximate nearest neighbors are found with constant probability (Section 5.6).

## 5.4 Improved Virtual Rehashing Strategy

In Section 3.2, we explained the original Virtual Rehashing strategy (denoted as *oVR* strategy) as proposed in C2LSH [13]. The initial radius is set to 1, and if sufficient results are not found, then the radius is increased in an exponential sequence:  $R = 1, c, c^2, c^3 \dots$  until sufficient number of results are found. The main drawback of this approach is when the values of  $R$  become larger (i.e. when the difference between two radius values is large - e.g. 4096 and 8192). In such situations, it happens frequently that very few (or no) nearest neighbor points are found at radius value 4096 but all (and lot more) are found at radius 8192. Thus, for example, if the actual radius of the  $k'$ th-nearest object was near 6000, then index files corresponding to radius 6000-8192 will be read unnecessarily from the disk, leading to expensive wasted IO operations. A recent work [23] has also attempted to solve this problem by recording closest object pairs in the projected distance. While this additional book-keeping does lead to savings in IO [23], the extra overhead

---

### Algorithm 1 k-Nearest Neighbor Object

---

```

1: Input: Object Query ( $Q$ ), Point queries belonging to  $Q$ 
   ( $set(Q)$ ), Number of layers ( $m$ ), Number of desired objects
   ( $k$ ),  $\Gamma$ -Threshold, Improved Initial Starting Radius ( $i2R$ ),
   Approximation Ratio ( $c$ )
2: Output: k-Nearest Neighbor Objects
3: Initialize:  $R = i2R$ , Candidate List  $\mathcal{CL} = \emptyset$ ,
    $numIter = 0$ 
4: procedure FINDKNNOBJECTS
5:   while TRUE do
6:     if  $|\{X_j | X_j \in \mathcal{CL} \wedge \Gamma dist(Q, X_j) \leq cR\}| \geq k$  then
7:       return the top- $k$  objects from  $\mathcal{CL}$ ;
8:     end if
9:     for  $g = 1$ ;  $g \leq m$ ;  $g++$  do
10:      for  $i = 1$ ;  $i \leq |set(Q)|$ ;  $i++$  do
11:        CountCollisions( $q_i$ );
12:         $\forall X_j \in S$  Update  $ci(Q, X_j)$ ;
13:      end for
14:      if  $|\mathcal{CL}| \geq k + \beta S$  then
15:        return the top- $k$  objects from  $\mathcal{CL}$ ;
16:      end if
17:    end for
18:     $R = R + c^{numIter}$ ;
19:     $numIter++$ ;
20:  end while
21: end procedure

```

---

is very expensive to compute and store. Instead, we design our improved Virtual Rehashing strategy (denoted as *iVR* strategy) based on the following observation:

**OBSERVATION 5.1.** *For high-dimensional datasets, the required radius values for a particular  $k'$  value are similar to each other for different query points for a given dataset.*

Figure 2 shows our observation on popular real high-dimensional datasets with varying cardinalities and dimensionalities (Audio [2], Color [10], Mnist [29], Sift [35]). For 1000 randomly chosen query points, we report the final radius values (using the Virtual Rehashing technique from C2LSH [13] and QALSH [16]) for top-100 points. This observation was also noted by a very recent paper [43] where the authors show that the homogeneity of the distance distributions of data points in different high-dimensional datasets is very high. By leveraging this simple observation, we design an improved, simple, and effective *Virtual Rehashing* technique: we execute a sample set of randomly chosen queries for a given  $k'$  and count the number of occurrences of the final radius value. We choose our initial radius value that is before the radius with the maximum count of sampled queries. E.g. in the Audio dataset (Figure 2), the radius with the maximum count is 8192. For these queries, it means that the optimal radius would be between 4096 and 8192. Hence we choose our initial radius value to be 4096. Thus instead of starting at the initial radius of 1, we find an improved initial starting radius (denoted as *i2R*) based on sampling queries at the end of the indexing process. Note that, since this is done during the indexing phase, it has no overhead during query execution. Additionally, we do not need to store any distance pairs, but simply need to execute a small number of top- $k'$  point queries to find the initial starting radius. Once the initial starting radius (*i2R*) is found, we leverage the same exponential sequence strategy

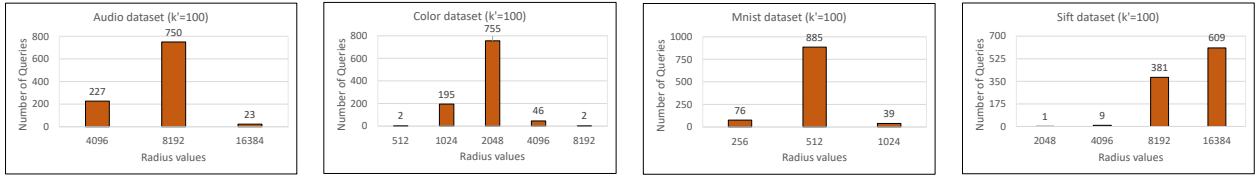


Figure 2: Final Radius Values for finding Top-100 Points for 1000 Point Queries on Different Datasets

as C2LSH, such that  $R = i2R+1, i2R+c, i2R+c^2, i2R+c^3 \dots$ . Thus, for 1000 random queries on the Audio dataset, using the original *Virtual Rehashing* technique, the average final radius is 7450 for  $c = 2$  and  $k' = 100$ . On the other hand, using our improved strategy, the average final radius is 6083, which leads to significant savings in the IO.

While these savings may not improve time in the order of magnitudes for a single point query, they do lead to significant performance improvement for an object query (which consists of hundreds of individual point queries). We experimentally show this in Section 6. Note that, one disadvantage of this approach is when there are queries that finish with a radius value much lower than the chosen initial radius. E.g., in the Color dataset (Figure 2), our strategy will choose  $i2R = 1024$ . As you can see, there were 2 out of 1000 queries whose final radius value to find top-100 points was 512. In this case, the *iVR* strategy will do wasted work by starting (and ending) at 1024. But when this is considered for an object query, the savings in the IO and time for majority of the point queries, belonging to the object query, offsets the wasted work for a very small number of queries.

**LEMMA 5.1.** *For majority of the queries, i.e., for those whose required radius in *oVR* is  $(2 \times i2R)$ , *iVR* strategy will generate less IOs than the *oVR* strategy.*

**PROOF.** Set  $R = i2R$ . Let  $Q$  be an object query and  $q_i \in \text{set}(Q)$ . Assume that the required radius in *oVR* is  $2R$ , that is, the actual radius  $r$  of the  $k'$ -th-nearest object satisfies  $R < r \leq 2R$ . In the *oVR*, the sequence of radii needed to find the  $k'$ -th-nearest object has  $\lfloor \log_2 R \rfloor + 2$  elements, that is,  $1, 2, 4, \dots, 2R$ . On the other hand, for the same query  $q$ , *iVR* analyzes at most  $\lfloor \log_2 R \rfloor + 1$  radii, that is,  $R+1, R+2, \dots, 2R$ . This finishes the proof.  $\square$

The *iVR* strategy is dependent on a given  $k'$ . For a lower  $k'$ , the final radius values will be lower than for a higher  $k'$ . Note that, *mmLSH* does not depend on any  $k'$  and instead depends on a  $\Gamma$ . The above strategy can be trivially extended to work with a  $\Gamma$  instead of a  $k'$ . We explain it for a  $k'$  because this can improve the performance of other LSH-based algorithms as well (such as C2LSH [13] and QALSH [16]) by reducing the overall IOs needed for query processing.

## 5.5 Advanced Buffer-conscious Strategy for Faster Query Processing

Another goal of *mmLSH* is to improve the processing speed of finding nearest neighbors of a given multimedia query object by efficiently utilizing a given buffer space. In order to explain our strategy, we first analyze the two expensive operations and the two naive strategies for solving the problem. The two main dominant costs in LSH-based techniques are the *Algorithm time* and the *Index IO time*:

- **Algorithm time** is the time required to complete processes such as finding the necessary index files (which are

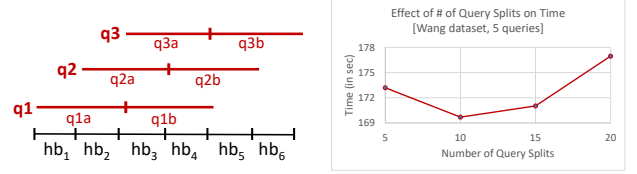


Figure 3: (a) Query Split Strategy, (b) Effect of # of Query Splits on Time

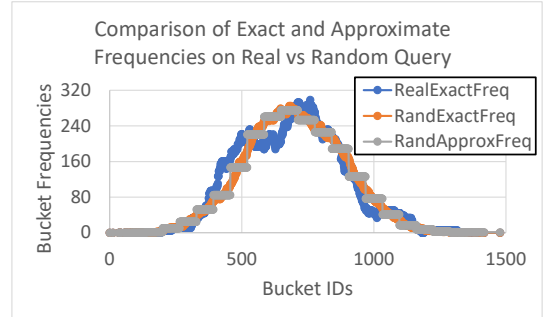


Figure 4: Comparison of Exact and Approximate Frequencies on a Real and Random Query

the hash buckets from the projections) and doing *Collision Counting* on these hash buckets to eventually find the candidate points that collide with the given query point.

- **Index IO time** is the time needed to bring the necessary index files (hash buckets) from the secondary storage to the primary storage (referred to as *buffer* in this paper).

The overall processing cost also includes cost of bringing necessary data candidate points into the buffer and computing the exact Euclidean distances to remove false positives, but these costs are very negligible (since the maximum number of accessed data points is  $k + v$  where  $v = 100$  in C2LSH [13]) and hence ignored in our following formulation. Due to space limitations, we do not present a formal cost model for this process. Our main focus is on minimizing the above mentioned two dominant costs: *algorithm time* and *index IO time*. We want to store the most important (and subsequently evict the least important) buckets from the buffer  $B$  such that the total number of buffer hits ( $B_{hits}$ ) are maximized (or buffer misses ( $B_{miss}$ ) are minimized).

- **Naive Strategy 1: Using LRU Eviction Strategy on a given buffer.** Given a query object  $Q$ , we first find the hash bucket locations for each of point queries of  $Q$ . In order to make the LRU (Least Recently Used) eviction strategy more effective, in each hash function  $m$ ,

	Total	AlgTime	IndexIOTime
NS1: LRU	263.6	117.6	146.0
NS2: Per-Bucket	279.5	260.8	18.7

Table 1: Performance Comparison of Naive Strategies (NS) 1 (LRU) and 2 (Per-Bucket) (in sec)

we order the execution of point queries of  $Q$  according to the hash bucket locations from left to right. During query processing, we evict the LRU index files from the buffer when the buffer gets full.

- **Naive Strategy 2: Using a Per-bucket Execution Strategy.** Since one of our goals is to reduce the *indexIO-Cost*, we also consider a Per-bucket execution strategy. Given a query object  $Q$ , we bring each useful hash bucket,  $hb$ , into the buffer, and for every  $q$  in  $Q$  that requires  $hb$ , we perform *Collision Counting* to find the candidate nearest neighbor points to the point query. In Figure 3, this strategy would bring in  $hb_1$  (then solve for  $q_1$ ), then bring  $hb_2$  (and then solve for  $q_1$  and  $q_2$ , since both queries using  $hb_2$ ) and so on.

As seen from Table 1, the above Naive Strategy 1 has a lot smaller Algorithm time cost than Naive Strategy 2, but the IndexIO time of the first strategy is a lot more than the IndexIO Time of the second strategy. The simplicity of Naive Strategy 1 results in a small Algorithm time cost. Naive Strategy 2, on the other hand, needs to find the queries that require the particular hash bucket brought into the main memory. While this process can be sped up with the use of additional index structures, it is still an expensive operation to check for all queries for each bucket, in each projection, for each radius. In each projection (in each radius), since a hash bucket is brought into the buffer only once for Strategy 2, the IndexIO time is the lowest.

Hence we propose an efficient and effective buffer-conscious strategy that reduces the IndexIO time of the first naive strategy without adding significant overhead to the Algorithm time (thus resulting in lower total time). Instead of using LRU, our eviction strategy is to evict a bucket based on the following three intuitive criteria. **Criterion 1:** if the bucket was not added to the buffer *very recently*. When a bucket is added to the buffer, then there is a high likelihood that another query might use it in the near future. **Criterion 2:** if the bucket is *far away* from the current query. It is more beneficial to evict another bucket that is far apart in the projection than the position of the current query. **Criterion 3:** if the number of queries that still require this bucket (called *frequency* of the bucket) in this radius is the lowest *after* the first two criteria are satisfied. Criterion 3 ensures that a bucket needed by a lot of queries is not evicted. Due to space limitations, we do not formally show the pseudo-code for the eviction process.

The main challenge in the above criteria is that the main criterion (Criterion 3) requires *mmLSH* to know the frequencies of each bucket in each projection at each radius to decide which bucket to evict. This is an unfair expensive requirement to have during online query processing. Across different real multimedia datasets, we observed that the frequencies of buckets on collection of queries associated with an object showed a behavior very similar to a collection of randomly chosen queries. Figure 4 shows that the bucket

frequencies for a randomly chosen query from the Wang [41] dataset exhibit a similar pattern for a set of randomly generated point queries on a single projection.

**Projection-Dividing Strategy:** We use this important observation to estimate the frequencies of buckets during offline processing. This step is merged with the *VR-Analyzer* and hence it does not incur any additional overhead. The necessary statistics are collected while the *VR-Analyzer* is running. Given a set of random point queries mapped to a projection, the following is the overview of our Projection-Dividing Strategy: 1) We divide a projection into different regions. 2) We calculate the average frequencies for the random point queries for each region, and assign the region’s frequency to each bucket in that particular region. 3) For each projection, we save this additional metadata in the index. Using the above strategy, we assign *approximate* frequencies to all buckets in each projection. The next technical challenge is to find how many regions to divide it in, and to decide the boundaries of the regions. For the first challenge, too few divisions will result in a high error between the estimated and actual frequencies. Too many divisions will also result in a high error because if the frequency behavior is slightly deviated than the random queries’ behavior, then we assign same frequencies as that of the random queries. We divide the projection into equal parts to find the boundaries.

**Query-Splitting Strategy:** We also noticed that when the radii are large and the buffer size is small, it is very difficult to effectively utilize the buffer for maximizing buffer hits. To alleviate this, we split the queries into multiple sub-queries and reorder the execution of the queries based on these new set of queries. In Figure 3 (a), the query execution order will change from  $q_1, q_2, q_3$  to  $q_1a, q_2a, q_1b, q_3a, q_2b, q_3b$  to utilize the buffer more effectively. Note that too many splits is still detrimental due to the increase in the overall Algorithm time (like Naive Strategy 2). Figure 3 (b) shows the effect of different number of splits on the overall time. In this work, we empirically find a good split (that is found during the indexing phase). We leave finding the optimal split using advanced cost models to future work.

## 5.6 Theoretical Analysis

### 5.6.1 Guarantees on the Stopping Conditions

The goal of this section is to prove the following theorem which provides a theoretical guarantee to *mmLSH*. For simplicity we perform the theoretical analysis for the case  $k = 1$ , the general case follows similarly after simple adaptations.

**THEOREM 5.1.** *Let  $Q$  be a query object and let*

$$L = \min\{|X| \mid X \in \mathcal{D}\}.$$

*If*

$$\Gamma \geq \sqrt{\max\left\{\frac{\ln \frac{1}{\delta}}{(\varepsilon - \delta)^2 |Q| L}, \frac{2 \ln \frac{2}{\beta}}{\beta^2 |Q| L}\right\}},$$

*then mmLSH finds a  $\Gamma$ - $c^2$ -approximate Nearest Neighbor with constant high probability.*

For the proof of this theorem we need the following lemma. For this, we consider the following two properties for a given query object  $Q$  and level  $R$ :

$\mathcal{P}1$ ) If  $X$  is an object such that  $\Gamma \text{dist}(Q, X) \leq R$  then  $X$  is a  $\Gamma$ -candidate.

$\mathcal{P}2$ ) The number of  $\Gamma$ -false positives is at most  $\beta S$ .

In the following lemma we show that the above properties hold with high probability.

LEMMA 5.2. *Let  $\delta$  be the probability defined in Section 3.2 and  $\varepsilon > \delta$  as defined in Section 5.2, then if*

$$\Gamma \geq \sqrt{\max \left\{ \frac{\ln \frac{1}{\delta}}{2(\varepsilon - \delta)^2 |Q||X|}, \frac{2 \ln \frac{2}{\beta}}{\beta^2 |Q||X|} \right\}}$$

we have  $\Pr[\mathcal{P}1] \geq 1 - \delta$  and  $\Pr[\mathcal{P}2] > \frac{1}{2}$ .

PROOF. For  $q_i \in \text{set}(Q)$  and  $x_j \in \text{set}(X)$ , let  $A$  be the condition  $cc(q, x_j) \geq l$ ,  $B$  be  $\|q, x_j\| \leq R$ , and  $C$  be  $\|q, x_j\| > cR$ . From the proof of Lemma 1 in [13] we know the following inequalities hold:

$$\Pr[A|B] \geq 1 - \delta \quad (5)$$

and

$$\Pr[\neg A|C] \geq (1 - \exp(-2(\alpha - p_2)^2 m)) \geq (1 - \frac{\beta}{2}). \quad (6)$$

We proceed to prove inequality  $\Pr[\mathcal{P}1] \geq 1 - \delta$ . Assume  $\Gamma \text{dist}(Q, X) \leq R$ , which is equivalent to

$$\Pr[\|q_i, x_j\| \leq R] \geq \Gamma,$$

where  $q_i \in \text{set}(Q)$  and  $x_j \in \text{set}(X)$ . Therefore,

$$p = \Pr[A] \geq \Pr[A \wedge B] = \Pr[A|B]\Pr[B] \geq (1 - \delta)\Gamma,$$

where the last inequality follows from Equation (5).

For every  $1 \leq i \leq |Q|$  and  $1 \leq j \leq |X|$ , let  $Y_{i,j} \sim \text{Ber}(1 - p)$  be a Bernoulli random variable which is equal to 1 if  $cc(q_i, x_j) < l$ . Then

$$\begin{aligned} \Pr[ci(Q, X) \geq (1 - \varepsilon)\Gamma] &= 1 - \Pr[\sum_{i,j} Y_{i,j} \\ &\geq (1 - (1 - \varepsilon)\Gamma)|Q||X|] \\ &\geq 1 - \exp(-2(p - (1 - \varepsilon)\Gamma)^2 |Q||X|) \\ &\geq 1 - \exp(-2(\varepsilon - \delta)^2 \Gamma^2 |Q||X|), \end{aligned}$$

where the second to last inequality follows from Hoeffding's Inequality. Therefore for the given range of  $\Gamma$  we have

$$\Pr[\mathcal{P}1] = \Pr[ci(Q, X) \geq (1 - \varepsilon)\Gamma] \geq 1 - \delta.$$

We continue with the proof of  $\Pr[\mathcal{P}2] > \frac{1}{2}$ . For this, we assume  $\Gamma \text{dist}(Q, X) > cR$ . Which is equivalent to

$$\Pr[\|q_i, x_j\| > cR] \geq 1 - \Gamma.$$

Then

$$\begin{aligned} 1 - p &= \Pr[\neg A] \geq \Pr[\neg A \wedge C] \\ &= \Pr[\neg A|C]\Pr[C] \\ &\geq (1 - \frac{\beta}{2})(1 - \Gamma) \end{aligned}$$

where the last inequality follows from Equation (6). Therefore,

$$p \leq 1 - (1 - \frac{\beta}{2})(1 - \Gamma) = \Gamma + \frac{\beta}{2} - \frac{\beta\Gamma}{2}.$$

For every  $1 \leq i \leq |Q|$  and  $1 \leq j \leq |X|$ , let  $Y_{i,j} \sim \text{Ber}(1 - p)$  be a Bernoulli random variable defined as above. Thus

$$\begin{aligned} \Pr[ci(Q, X) \geq \Gamma + \frac{\beta}{2}] \\ &= \Pr[\sum_{i,j} Y_{i,j} < (1 - \Gamma - \frac{\beta}{2})|Q||X|] \\ &= \Pr[\sum_{i,j} Y_{i,j} \leq (1 - \Gamma - \frac{\beta}{2} - \Delta)|Q||X|] \end{aligned}$$

for some  $\Delta > 0$ . Thus, from Hoeffding's Inequality it follows that

$$\begin{aligned} q &= \Pr[ci(Q, X) \geq \Gamma + \frac{\beta}{2}] \\ &\leq \exp(-2(\Gamma + \frac{\beta}{2} + \Delta - p)^2 |Q||X|) \\ &< \exp(-2(\Gamma + \frac{\beta}{2} - p)^2 |Q||X|) \\ &\leq \exp(-2(\frac{\beta}{2})^2 \Gamma^2 |Q||X|). \end{aligned}$$

Let  $FP$  be the set of false positives, that is

$$FP = \{X \in \mathcal{D} \mid ci(Q, X) \geq \Gamma + \frac{\beta}{2} \text{ and } \Gamma \text{dist}(Q, X) > cR\},$$

then  $\Pr[\mathcal{P}2] = \Pr[|FP| \leq \beta S]$ . Therefore, it suffices to show the latter is larger than  $\frac{1}{2}$ .

Let  $X_1, \dots, X_S$  denote the elements of  $\mathcal{D}$ . For every  $1 \leq i \leq S$  let  $Z_i \sim \text{Ber}(q)$  be the Bernoulli random variable which is equal to one if  $X_i \in FP$ . Then the expected value of the size of  $FP$  satisfies

$$\begin{aligned} E(|FP|) &= E(\sum_i Z_i) = \sum_i E(Z_i) \\ &= S \cdot q < S \cdot \exp(-2(\frac{\beta}{2})^2 \Gamma^2 |Q||X|). \end{aligned}$$

Therefore, from Markov's Inequality it follows that

$$\begin{aligned} \Pr[|FP| \leq \beta S] &= 1 - \Pr[|FP| > \beta S] \\ &\geq \frac{E[|FP|]}{\beta S} \\ &> 1 - \frac{1}{\beta} \exp(-2(\frac{\beta}{2})^2 \Gamma^2 |Q||X|) \geq \frac{1}{2}, \end{aligned}$$

where the last inequality holds by the assumption on  $\Gamma$ . This finishes the proof.  $\square$

We are now ready to prove the theorem.

PROOF OF THEOREM 5.1. By Lemma 5.2 properties  $\mathcal{P}1$  and  $\mathcal{P}2$  hold with constant high probability. Therefore, we may assume these properties hold simultaneously.

Let  $r$  be the smallest  $\Gamma$ -distance between  $Q$  and an object of  $\mathcal{D}$ . Set  $t = \lceil \log_e r \rceil$  and  $R = c^t$ .

Assume first that the algorithm finishes with terminating condition  $\mathcal{T}1$ , that is at level  $R$  at least  $1 + \beta S$   $\Gamma$ -candidates have been found. By property  $\mathcal{P}2$  at most  $\beta S$  of these are false positives. Let  $X$  be the object returned by the algorithm, then we have  $\Gamma \text{dist}(Q, X) \leq cR \leq c^2 r$ .

Now, if the algorithm does not finish with  $\mathcal{T}1$ , then property  $\mathcal{P}2$  guarantees it finishes with  $\mathcal{T}2$  at the end of level  $R$ . Let  $X$  be the object returned by the algorithm, then we have  $\Gamma \text{dist}(Q, X) \leq R \leq cr < c^2 r$ . This finishes the proof.  $\square$

Dataset	$n \times 10^6$	$d$	Objects	Features
Caltech [8]	3.8	32	28,049	Brief[7]
Corel [11]	1.7	64	9,994	Surf[4]
MirFlicker [28]	12.0	32	24,980	ORB[33]
Wang [41]	0.7	128	1,000	Sift[25]

Table 2: Datasets

Parameter	Value range
# of Desired Objects ( $k$ )	5; <b>25</b> ; 50;
Buffer size (in MB)	20; <b>30</b> ; 50;
# of Query Splits	5; <b>10</b> ; 20;

Table 3: Parameters and Default Values (in bold)

## 6. EXPERIMENTAL EVALUATION

In this section, we evaluate the effectiveness of our proposed index structure, *mmLSH* on four real multimedia data sets, under different system parameters. All experiments were run on the nodes of the Bigdat cluster<sup>4</sup> with the following specifications: two Intel Xeon E5-2695, 256GB RAM, 1TB SSD, and CentOS 6.5 operating system. We used the state-of-the-art C2LSH [13] as our base implementation.<sup>5</sup> One limitation of C2LSH is that it stores all index files in memory. In order to make our work scalable to very large datasets, we modified the code such that the index files are stored on the secondary storage, and they are accessed from the secondary storage when needed. All codes were written in C++11 and compiled with gcc v4.7.2 with the -O3 optimization flag. For existing state-of-the-art algorithms (C2LSH and QALSH), we used the Borda Count process (Section 5.1), to aggregate the results of the point queries to find the nearest neighbor objects. Additionally, since the accuracy and the performance of the aggregation is affected by the chosen number of top- $k'$  results of the point queries, we choose a varying  $k'$  for Linear, C2LSH, and QALSH for a fair comparison:  $k' = 25, 50, 100$ . We also implement an LRU buffer for the indexes in C2LSH and QALSH to show a fair comparison with our results. We compare our work with the following alternatives:

- **LinearSearch-Borda:** In this alternative, the top- $k'$  results of the point queries are found using a brute-force linear search. This method does not utilize the buffer since it does not have any indexes.
- **C2LSH-Borda:** The top- $k'$  results of the point queries are found using the C2LSH [13] algorithm.
- **QALSH-Borda:** The top- $k'$  results of the point queries are found using the QALSH [16] algorithm.

### 6.1 Datasets

We use four real multimedia datasets to evaluate *mmLSH*. We used different feature extraction algorithms on these datasets to show the effectiveness of *mmLSH*. The details of these datasets are listed in Table 2.

<sup>4</sup>Supported by NSF Award #1337884

<sup>5</sup>*mmLSH* can be implemented over any state-of-the-art LSH technique.

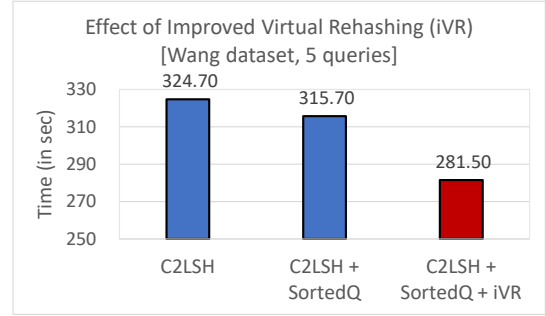


Figure 5: Comparison of C2LSH Original Virtual Rehashing (oVR) vs our Improved Virtual Rehashing (iVR)

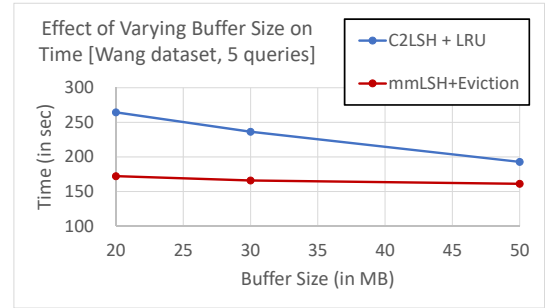


Figure 6: Effect of Buffer Size on Time

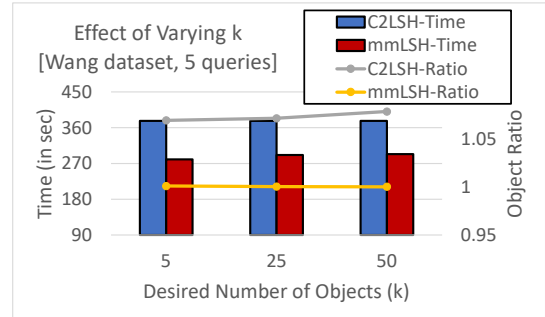


Figure 7: Effect of Varying  $k$

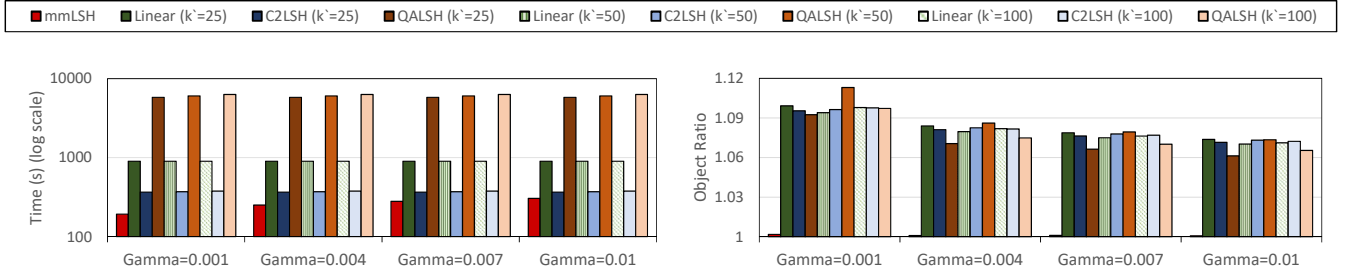


Figure 8: Comparison of Time and Accuracy of *mmLSH* against alternatives on *Wang* dataset

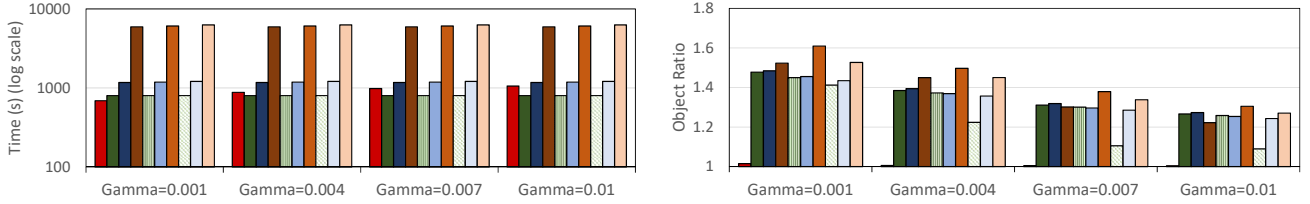


Figure 9: Comparison of Time and Accuracy of *mmLSH* against alternatives on *Corel* dataset

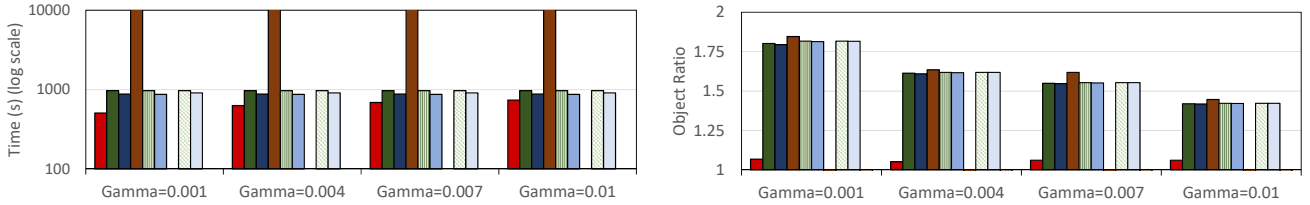


Figure 10: Comparison of Time and Accuracy of *mmLSH* against alternatives on *Caltech* dataset

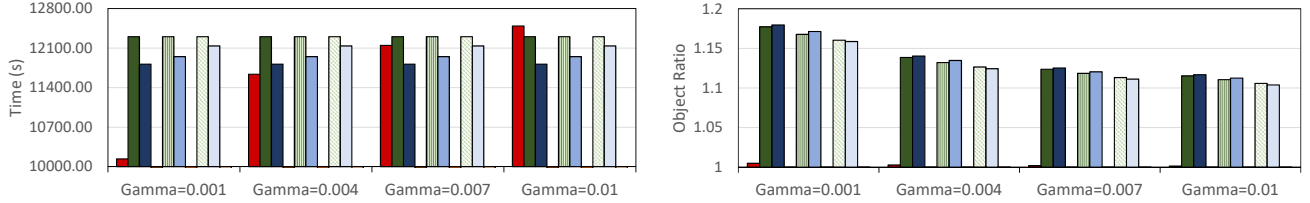


Figure 11: Comparison of Time and Accuracy of *mmLSH* against alternatives on *MirFlickr* dataset

- **Caltech**[8] This dataset consists of 3,767,761 32-dimensional points that were created using BRIEF [7] on 28,049 images belonging to 256 categories.
- **Corel**[11] This dataset consists of 1,710,725 64-dimensional points that were created using SURF [4] on 9,994 images belonging to 100 categories.
- **MirFlickr**[28] This dataset consists of 12,004,143 32-dimensional points that were created using ORB [33] on 24,980 images.
- **Wang**[41] This dataset consists of 695,672 128-dimensional SIFT descriptors [25] belonging to 1000 images. These images belong to 10 different categories; each category has 100 similar images.

## 6.2 Evaluation Criteria and Parameters

We evaluate the execution time and accuracy of *mmLSH* using the following criteria:

- **Time:** The two main dominant costs in LSH-based techniques are the algorithm time and the index IO time. We observed that the index IO times were not consistent (i.e. running the same query multiple times, which needed the same index IOs, would return drastically different results, mainly because of disk cache and instruction cache issues). Hence, we simulated the index IO time by benchmarking the read speed of our hard-disk (181 MB/s).
- **Accuracy:** Similar to the ratio defined in earlier works [39, 36, 24, 13, 16], we define an object ratio to calculate the accuracy of the returned top- $k$  objects as following:

$$OR_{\Gamma}(Q) = \frac{1}{k} \sum_{i=1}^k \frac{\Gamma dist(Q, X_i)}{\Gamma dist(Q, X_i^*)} \quad (7)$$

where  $X_1, \dots, X_k$  denote the top- $k$  objects returned from the algorithm and  $X_1^*, \dots, X_k^*$  denote the real objects found from the ground truth.  $\Gamma dist$  is computed using Equation 3. Object Ratio of 1 shows that the accuracy is 100% and as this value increases, the accuracy becomes lower.

We do not report the index size or the index construction cost, since they would be the same as the underlying LSH implementation that we use (C2LSH [13]). Table 3 shows our default parameter settings and the different ranges that we consider. We choose  $\delta = 0.1$ ,  $\beta = \frac{25}{S}$ ,  $\varepsilon = 0.2$ ,  $w = 2.184$  [16] for C2LSH and mmLSH,  $w = 2.7191$  [16] for QALSH. We randomly chose 10 multimedia objects as queries from each dataset and report the average of the results.

### 6.3 Discussion of the Results

In this section, we analyze the execution time and accuracy of *mmLSH* using the criteria explained in Section 6.2 against its alternatives. We note that QALSH gives drastically worse times than C2LSH, and hence when comparing the effectiveness for varying parameters, we only compare with C2LSH. In Section 6.3.4, we compare against all alternatives.

#### 6.3.1 Effect of our improved Virtual Rehashing (iVR)

In Figure 5, we show the effect of our improved Virtual Rehashing (iVR) technique (Section 5.4). In this figure, *C2LSH* represents the original code, *C2LSH + SortedQ* represents the code where the point queries are executed in sorted order of their hash values in each projection, and *C2LSH + SortedQ + iVR* represents C2LSH + our iVR technique. This figure does not show any buffer experiments so that we can isolate and understand the effect of iVR. This figure shows that our iVR technique improves the time by  $\approx 13\%$  for the Wang dataset. We notice similar gains on other datasets as well, but we do not show these results due to space limitations.

#### 6.3.2 Effect of Buffer Size

Figure 6 shows the benefit of our eviction strategy (Section 5.5) when compared with C2LSH + LRU for varying buffer sizes. It is evident from this figure that our three criterion are helpful in evicting the less useful index files (and keeping the more useful files in the buffer). The small overhead in Algorithm time is offset by a significant reduction in the number of index IOs, which eventually results in lower overall time. We found out that the highest L3 cache size is 24.75 MB for desktop processors and 60MB for server processors. Therefore, we decided to choose the buffer sizes between 20 MB and 50 MB in this figure.

#### 6.3.3 Effect of Number of Desired Objects

Figure 7 shows the execution time and accuracy of *mmLSH* against C2LSH for varying number of desired objects ( $k$ ). This figure shows that *mmLSH* has better time and object ratio for different  $k$  values. Additionally, it shows that *mmLSH* is scalable for a large number of desired objects as well. Results show that by increasing  $k$ , the execution time of both algorithms increase by only 0.33%. Moreover, although the object ratio of *mmLSH* stays the same by increasing  $k$ , the object ratio of C2LSH increases considerably.

#### 6.3.4 Comparison of *mmLSH* vs. State-of-the-art Methods on Different Datasets












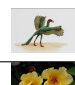




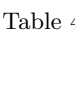


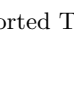






Query	mmLSH	Linear	C2LSH	QALSH
	  	  	  	  
	  	  	  	  

Table 4: Sorted Top-3 Images

In this section, we compare *mmLSH* with all alternatives on different datasets. Figures 8 9, 10, 11 show the performance and accuracy of *mmLSH*, LinearSearch-Borda, C2LSH-Borda, QALSH-Borda for 4 real multimedia datasets with varying characteristics. Note that the Borda count process is done after query processing and takes very negligible time. We found that QALSH took a very long time as compared with *mmLSH* and other alternatives. Even a single query had not finished for more than 40 hours, and hence we choose not to report it for the largest dataset in our experiments (MirFlickr). *mmLSH* always returns a higher accuracy than the alternatives while being much faster than all three alternatives. One important point to note is the scalability of LSH-based algorithms for very large-scale datasets such as MirFlickr (where the query time is  $>10k$  seconds). In our work, we consider all feature-vectors that are extracted by a feature-extraction algorithm. Several works [38, 21] have been proposed that cluster these points with the purpose of finding a representative point to reduce the complexity of the problem.

#### 6.3.5 Comparison of Top-3 Images

In Table 4, we show the top-3 nearest neighbors for two image queries on the Wang dataset. *mmLSH* returns all 3 images close to the query images. However, the alternative algorithms return false positives for the first query. Also, although the second query is a single flower, the alternative algorithms return images composed of two flowers as their top-1 result.

## 7. CONCLUSION

In this paper, we presented a novel index structure for efficiently finding top- $k$  approximate nearest neighbors for multimedia data using LSH, called *mmLSH*. In *mmLSH*, we present novel strategies that improve the execution time and accuracy for a given multimedia object query. Additionally, we provide rigorous theoretical analysis and guarantees on our returned results. Experimental evaluation shows the benefit of *mmLSH* in terms of execution time and accuracy compared to state of the art algorithms.

## 8. REFERENCES

- [1] A. Arora, S. Sinha, P. Kumar, and A. Bhattacharya. Hd-index: Pushing the scalability-accuracy boundary for approximate knn search in high-dimensional spaces. *Proc. VLDB Endow.*, 11(8):906–919, Apr. 2018.
- [2] Audio dataset. <http://www.cs.princeton.edu/cass/audio.tar.gz>.
- [3] M. Bawa, T. Condie, and P. Ganesan. Lsh forest: Self-tuning indexes for similarity search. In *Proceedings of the 14th International Conference on World Wide Web*, WWW '05, pages 651–660, New York, NY, USA, 2005. ACM.
- [4] H. Bay, T. Tuytelaars, and L. Van Gool. Surf: Speeded up robust features. In A. Leonardis, H. Bischof, and A. Pinz, editors, *Computer Vision – ECCV 2006*, pages 404–417, Berlin, Heidelberg, 2006. Springer Berlin Heidelberg.
- [5] J. L. Bentley. Multidimensional binary search trees used for associative searching. *Commun. ACM*, 18(9):509517, Sept. 1975.
- [6] S. N. Borade, R. R. Deshmukh, and S. Ramu. Face recognition using fusion of pca and lda: Borda count approach. In *2016 24th Mediterranean Conference on Control and Automation (MED)*, pages 1164–1167, June 2016.
- [7] M. Calonder, V. Lepetit, C. Strecha, and P. Fua. Brief: Binary robust independent elementary features. In *European conference on computer vision*, pages 778–792. Springer, 2010.
- [8] Caltech dataset. [http://www.vision.caltech.edu/Image\\_Datasets/Caltech256](http://www.vision.caltech.edu/Image_Datasets/Caltech256).
- [9] E. Chávez, G. Navarro, R. Baeza-Yates, and J. L. Marroquín. Searching in metric spaces. *ACM Comput. Surv.*, 33(3):273–321, Sept. 2001.
- [10] Color dataset. <http://kdd.ics.uci.edu/databases/CorelFeatures>.
- [11] Corel dataset. <http://www.ci.gxnu.edu.cn/cbir/Dataset.aspx>.
- [12] M. Datar, N. Immorlica, P. Indyk, and V. S. Mirrokni. Locality-sensitive hashing scheme based on p-stable distributions. In *Proceedings of the Twentieth Annual Symposium on Computational Geometry*, SCG '04, pages 253–262, New York, NY, USA, 2004. ACM.
- [13] J. Gan, J. Feng, Q. Fang, and W. Ng. Locality-sensitive hashing scheme based on dynamic collision counting. In *Proceedings of the 2012 ACM SIGMOD International Conference on Management of Data*, SIGMOD '12, pages 541–552, New York, NY, USA, 2012. ACM.
- [14] J. Gao, H. Jagadish, B. C. Ooi, and S. Wang. Selective hashing: Closing the gap between radius search and k-nn search. In *Proceedings of the 21th ACM SIGKDD International Conference on Knowledge Discovery and Data Mining*, KDD '15, pages 349–358, New York, NY, USA, 2015. ACM.
- [15] A. Gionis, P. Indyk, and R. Motwani. Similarity search in high dimensions via hashing. In *Proceedings of the 25th International Conference on Very Large Data Bases*, VLDB '99, pages 518–529, San Francisco, CA, USA, 1999. Morgan Kaufmann Publishers Inc.
- [16] Q. Huang, J. Feng, Y. Zhang, Q. Fang, and W. Ng. Query-aware locality-sensitive hashing for approximate nearest neighbor search. *Proc. VLDB Endow.*, 9(1):1–12, Sept. 2015.
- [17] O. Jafari, J. Ossorgin, and P. Nagarkar. qwlsh: Cache-conscious indexing for processing similarity search query workloads in high-dimensional spaces. In *Proceedings of the 2019 on International Conference on Multimedia Retrieval*, ICMR '19, pages 329–333, New York, NY, USA, 2019. ACM.
- [18] H. Jégou, M. Douze, and C. Schmid. Improving bag-of-features for large scale image search. *Int. J. Comput. Vision*, 87(3):316–336, May 2010.
- [19] H. Jgou, M. Douze, and C. Schmid. Packing bag-of-features. In *2009 IEEE 12th International Conference on Computer Vision*, pages 2357–2364, Sep. 2009.
- [20] N. Katayama and S. Satoh. The sr-tree: An index structure for high-dimensional nearest neighbor queries. *SIGMOD Rec.*, 26(2):369380, June 1997.
- [21] J. Krizaj, V. Štruc, and N. Pavešić. Adaptation of sift features for robust face recognition. In A. Campilho and M. Kamel, editors, *Image Analysis and Recognition*, pages 394–404, Berlin, Heidelberg, 2010. Springer Berlin Heidelberg.
- [22] W. Li, Y. Zhang, Y. Sun, W. Wang, M. Li, W. Zhang, and X. Lin. Approximate nearest neighbor search on high dimensional data - experiments, analyses, and improvement. *IEEE Transactions on Knowledge and Data Engineering*, pages 1–1, 2019.
- [23] W. Liu, H. Wang, Y. Zhang, W. Wang, and L. Qin. I-lsh: I/o efficient c-approximate nearest neighbor search in high-dimensional space. In *2019 IEEE 35th International Conference on Data Engineering (ICDE)*, pages 1670–1673, April 2019.
- [24] Y. Liu, J. Cui, Z. Huang, H. Li, and H. T. Shen. Sk-lsh: An efficient index structure for approximate nearest neighbor search. *Proc. VLDB Endow.*, 7(9):745–756, May 2014.
- [25] D. G. Lowe. Distinctive image features from scale-invariant keypoints. *International Journal of Computer Vision*, 60(2):91–110, Nov 2004.
- [26] A. Lumini and L. Nanni. Detector of image orientation based on borda count. *Pattern Recognition Letters*, 27(3):180 – 186, 2006.
- [27] Q. Lv, W. Josephson, Z. Wang, M. Charikar, and K. Li. Multi-probe lsh: Efficient indexing for high-dimensional similarity search. In *Proceedings of the 33rd International Conference on Very Large Data Bases*, VLDB '07, pages 950–961. VLDB Endowment, 2007.
- [28] MirFlicker dataset. <http://press.liacs.nl/mirflickr>.
- [29] Mnist dataset. <http://yann.lecun.com/exdb/mnist>.
- [30] P. Nagarkar and K. S. Candan. Psish: An index structure for efficient execution of set queries in high-dimensional spaces. In *Proceedings of the 27th ACM International Conference on Information and Knowledge Management*, CIKM '18, pages 477–486, New York, NY, USA, 2018. ACM.
- [31] C. A. Perez, L. A. Cament, and L. E. Castillo. Methodological improvement on local gabor face recognition based on feature selection and enhanced

- borda count. *Pattern Recognition*, 44(4):951 – 963, 2011.
- [32] B. Reilly. Social choice in the south seas: Electoral innovation and the borda count in the pacific island countries. *International Political Science Review*, 23(4):355–372, 2002.
- [33] E. Rublee, V. Rabaud, K. Konolige, and G. Bradski. Orb: An efficient alternative to sift or surf. In *2011 International conference on computer vision*, pages 2564–2571. Ieee, 2011.
- [34] Seyoon Jeong, Kyuheon Kim, Byungtae Chun, Jaeyeon Lee, and Y. J. Bae. An effective method for combining multiple features of image retrieval. In *Proceedings of IEEE. IEEE Region 10 Conference. TENCON 99. 'Multimedia Technology for Asia-Pacific Information Infrastructure' (Cat. No.99CH37030)*, volume 2, pages 982–985 vol.2, Sep. 1999.
- [35] Sift dataset. <http://corpus-texmex.irisa.fr>.
- [36] Y. Sun, W. Wang, J. Qin, Y. Zhang, and X. Lin. Srs: Solving c-approximate nearest neighbor queries in high dimensional euclidean space with a tiny index. *Proc. VLDB Endow.*, 8(1):1–12, Sept. 2014.
- [37] N. Sundaram, A. Turmukhametova, N. Satish, T. Mostak, P. Indyk, S. Madden, and P. Dubey. Streaming similarity search over one billion tweets using parallel locality-sensitive hashing. *Proc. VLDB Endow.*, 6(14):1930–1941, Sept. 2013.
- [38] C. Tao, Y. Tan, H. Cai, and J. Tian. Airport detection from large ikonos images using clustered sift keypoints and region information. *IEEE Geoscience and Remote Sensing Letters*, 8(1):128–132, Jan 2011.
- [39] Y. Tao, K. Yi, C. Sheng, and P. Kalnis. Efficient and accurate nearest neighbor and closest pair search in high-dimensional space. *ACM Trans. Database Syst.*, 35(3):20:1–20:46, July 2010.
- [40] G. Tzanetakis and P. Cook. Marsyas: A framework for audio analysis. *Org. Sound*, 4(3):169–175, Dec. 1999.
- [41] J. Z. Wang, Jia Li, and G. Wiederhold. Simplicity: semantics-sensitive integrated matching for picture libraries. *IEEE Transactions on Pattern Analysis and Machine Intelligence*, 23(9):947–963, Sep. 2001.
- [42] W. Zhang, K. Gao, Y.-d. Zhang, and J.-t. Li. Data-oriented locality sensitive hashing. In *Proceedings of the International Conference on Multimedia*, MM '10, pages 1131–1134, New York, NY, USA, 2010. ACM.
- [43] B. Zheng, X. Zhao, L. Weng, N. Q. V. Hung, H. Liu, and C. S. Jensen. Pm-lsh: A fast and accurate lsh framework for high-dimensional approximate nn search. *Proc. VLDB Endow.*, 13(5):643655, Jan. 2020.
- [44] Zhong Wu, Qifa Ke, M. Isard, and Jian Sun. Bundling features for large scale partial-duplicate web image search. In *2009 IEEE Conference on Computer Vision and Pattern Recognition*, pages 25–32, June 2009.
- [45] W. Zhou, H. Li, Y. Lu, and Q. Tian. Large scale image search with geometric coding. In *Proceedings of the 19th ACM International Conference on Multimedia*, MM '11, pages 1349–1352, New York, NY, USA, 2011. ACM.